JACS
JOURNAL OF THE AMERICAN CHEMICAL SOCIETY
Communication
pubs.acs.org/JACS

Direct Observation of Key Catalytic Intermediates in a Photoinduced Proton Reduction Cycle with a Diiron Carbonyl Complex

Mohammad Mirmohades,[§] Sonja Pullen,[§,‡] Matthias Stein,[‡] Somnath Maji,[§] Sascha Ott,[§] Leif Hammarström,[§] and Reiner Lomoth*[,§]

[§]Ångström Laboratory, Department of Chemistry, Uppsala University, Box 523, 75120 Uppsala, Sweden
[‡]Max Planck Institute for Dynamics of Complex Technical Systems, Sandtorstraße 1, 39106 Magdeburg, Germany

Supporting Information

ABSTRACT: The structure and reactivity of intermediates in the photocatalytic cycle of a proton reduction catalyst, $[Fe_2(bdt)(CO)_6]$ (bdt = benzenedithiolate), were investigated by time-resolved spectroscopy. The singly reduced catalyst $[Fe_2(bdt)(CO)_6]^-$, a key intermediate in photocatalytic H_2 formation, was generated by reaction with one-electron reductants in laser flash-quench experiments and could be observed spectroscopically on the nanoseconds to microseconds time scale. From UV/vis and IR spectroscopy, $[Fe_2(bdt)(CO)_6]^-$ is readily distinguished from the two-electron reduced catalyst $[Fe_2(bdt)(CO)_6]^{2-}$ that is obtained inevitably in the electrochemical reduction of $[Fe_2(bdt)(CO)_6]$. For the disproportionation rate constant of $[Fe_2(bdt)(CO)_6]^-$, an upper limit on the order of 10^7 M^{-1} s^{-1} was estimated, which precludes a major role of $[Fe_2(bdt)(CO)_6]^{2-}$ in photoinduced proton reduction cycles. Structurally $[Fe_2(bdt)(CO)_6]^-$ is characterized by a rather asymmetrically distorted geometry with one broken Fe−S bond and six terminal CO ligands. Acids with $pK_a \leq 12.7$ protonate $[Fe_2(bdt)(CO)_6]^-$ with bimolecular rate constants of 4×10^6, 7×10^6, and 2×10^8 M^{-1} s^{-1} (trichloroacetic, trifluoroacetic, and toluenesulfonic acids, respectively). The resulting hydride complex $[Fe_2(bdt)(CO)_6H]$ is therefore likely to be an intermediate in photocatalytic cycles. This intermediate resembles structurally and electronically the parent complex $[Fe_2(bdt)(CO)_6]$, with very similar carbonyl stretching frequencies.

Catalysts for multi-electron redox reactions are essential components of prospective chemical energy storage and conversion technology. Thus, the design of molecular catalysts for reactions like H_2 formation attracts extensive attention.[1] However, characterization of catalytic reactivity is usually limited to the measurement of catalytic currents or rates of H_2 formation in electrochemical or photochemical proton reduction. Even where these quantities are actually limited by the catalytic reaction, they can only reveal effective turnover frequency (TOF) for the catalytic cycle under the conditions of the experiment. The mechanism, the nature of the rate-determining step, and the TOF may in general vary depending on reaction conditions. Instead, kinetic information on the different catalytic steps under relevant conditions is required for proper understanding and performance evaluation. Direct observation of catalytic intermediates and the kinetics of their transformations is usually impeded by the rapid turnover of more efficient catalysts. With regard to H_2 formation catalysts, spectroscopic observation of species pertinent to the catalytic cycle was mostly restricted to initial reduction or protonation products obtained under non-catalytic conditions, like the examples given in ref 2. Direct spectroscopic observations of reduced protonated species are scarce and limited to rather unreactive examples.[3] Here we report on the spectroscopic and kinetic characterization of intermediates in the photocatalytic cycle of $[Fe_2(bdt)(CO)_6]$ (bdt = benzenedithiolate),[4] which is a prototypical proton reduction catalyst based on the active-site structure of FeFe-hydrogenases. Electrochemical H_2 formation with this catalyst proceeds via initial two-electron ($2e^-$) reduction of $[Fe_2(bdt)(CO)_6]$ and subsequent protonation of $[Fe_2(bdt)(CO)_6]^{2-}$ (Scheme 1).[5] However, this mechanism is unlikely to apply to photocatalytic H_2 formation, which relies on photoinduced one-electron ($1e^-$) reduction steps. In this study, the relevant $1e^-$ reduction step was triggered by laser flash-quench methods. Combining this approach with a recently developed technique for time-resolved infrared spectroscopy[6] resulted in the first IR spectroscopic characterization of reduced and protonated intermediates of a H_2 formation catalyst with nanosecond time resolution. Direct observation of $[Fe_2(bdt)(CO)_6]^-$ and its protonation product $[Fe_2(bdt)(CO)_6H]$ by IR spectroscopy revealed important kinetic and structural characteristics of these key intermediates.

Scheme 1. One-Electron Reduction and Subsequent Protonation of $[Fe_2(bdt)(CO)_6]$

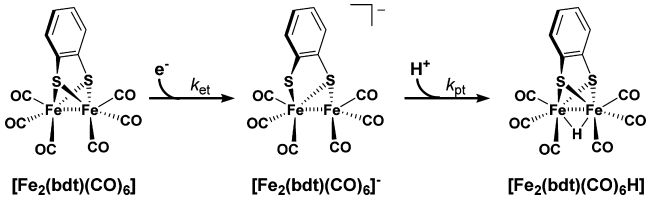

Reduction of $[Fe_2(bdt)(CO)_6]$ was accomplished by electron transfer from $[Ru(dmb)_3]^+$ (dmb = 4,4′-dimethyl-2,2′-bipyridine).[7] The reductant ($E^0 = -1.71$ V vs ferrocene in acetonitrile) was obtained by reductive quenching of the photoexcited sensitizer $[Ru(dmb)_3]^{2+}$ with tetrathiafulvalene (TTF) (see Supporting Information (SI) for details) and reacts with

Received: August 20, 2014
Published: November 24, 2014

   dx.doi.org/10.1021/ja5085817 | J. Am. Chem. Soc. 2014, 136, 17366−17369

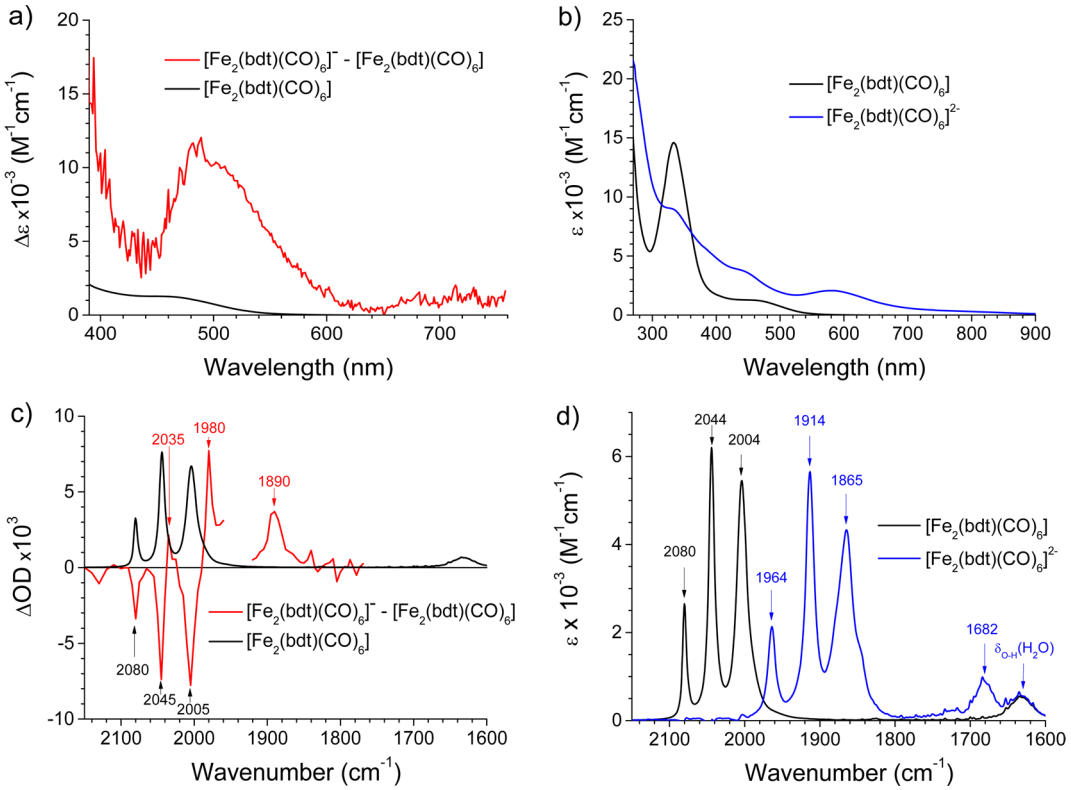

Figure 1. UV/vis and IR spectra of $[Fe_2(bdt)(CO)_6]^{n-}$ (n = 0, 1, 2) in acetonitrile. (a) UV/vis transient absorption spectrum of $[Fe_2(bdt)(CO)_6]^-$ obtained by reduction of $[Fe_2(bdt)(CO)_6]$ with flash-quench generated $[Ru(dmb)_3]^+$ 10 μs after excitation. (b) UV/vis spectra of $[Fe_2(bdt)(CO)_6]$ and electrochemically generated $[Fe_2(bdt)(CO)_6]^{2-}$ (−1.8 V vs Fc). (c) IR transient absorption spectrum of $[Fe_2(bdt)(CO)_6]^-$ obtained by reduction of $[Fe_2(bdt)(CO)_6]$ with flash-quench generated $[Ru(dmb)_3]^+$ 1−2 μs after excitation. (d) IR spectra of $[Fe_2(bdt)(CO)_6]$ and electrochemically generated $[Fe_2(bdt)(CO)_6]^{2-}$ (−1.8 V vs Fc). Conditions: (a) 590 μM $[Fe_2(bdt)(CO)_6]$, 1.6 mM TTF, 40 μM $[Ru(dmb)_3]^{2+}$, λ_{ex} = 532 nm, fwhm = 10 ns, 10 mJ/pulse; (b) 1.9 mM $[Fe_2(bdt)(CO)_6]$, 0.1 M $TBAPF_6$; (c) 1.3 mM $[Fe_2(bdt)(CO)_6]$, 3.8 mM TTF, 200 μM $[Ru(dmb)_3]^{2+}$, λ_{ex} = 532 nm, fwhm = 10 ns, 10 mJ/pulse; (d) 1.4 mM $[Fe_2(bdt)(CO)_6]$, 0.1 M $TBAPF_6$.

$[Fe_2(bdt)(CO)_6]$ at an almost diffusion-controlled rate ($k_{et} = 5 \times 10^9$ M^{-1} s^{-1}). The product spectrum (Figure 1a) features a pronounced absorption band centered at ∼500 nm that can be assigned to the 1e$^-$ reduced catalyst. A recent study on photoinduced reduction of $[Fe_2(bdt)(CO)_6]$ reported a band at 570 nm that was observed in post-illumination steady-state absorption spectra and assigned to $[Fe_2(bdt)(CO)_6]^-$.[8] Comparison to Figure 1a shows, however, that the reported absorption band cannot arise from $[Fe_2(bdt)(CO)_6]^-$. $[Fe_2(bdt)(CO)_6]^-$ is re-oxidized to $[Fe_2(bdt)(CO)_6]$ in the diffusion-controlled recombination with the TTF radical cation,[9] while no signs for disproportionation can be observed. The 2e$^-$ reduced catalyst $[Fe_2(bdt)(CO)_6]^{2-}$ would be readily detected by its distinctively different absorption spectrum (Figure 1b) with prominent bands at 450 and 580 nm. However, even in complementary flash-quench experiments with sacrificial electron donor (SI),[10] where $[Fe_2(bdt)(CO)_6]^-$ persisted on the time scale of seconds, no formation of $[Fe_2(bdt)(CO)_6]^{2-}$ was detected, which puts an upper limit on the order of 10^7 M^{-1} s^{-1} on the rate constant of disproportionation. The formation of the 2e$^-$ reduced catalyst by disproportionation of $[Fe_2(bdt)(CO)_6]^-$ is hence kinetically disfavored relative to the faster recombination reaction and in particular will not be able to compete with the pseudo-first-order kinetics of protonation of $[Fe_2(bdt)(CO)_6]^-$ with excess acid (see below). These results support the notion that $[Fe_2(bdt)(CO)_6]^-$ will be the dominant reduced state under the conditions of photoinduced H_2 formation.

For further characterization of this key intermediate, analogous flash-quench measurements with IR detection[6] were performed. The spectra were generated point by point from single-wavenumber kinetic traces that were averages of single flash experiments. Figure 1c shows a transient absorption spectrum in the carbonyl (CO) region that was recorded after reduction of $[Fe_2(bdt)(CO)_6]$ with flash-quench generated $[Ru(dmb)_3]^+$. The difference spectrum shows bleaching of all three ν_{C-O} bands (2004, 2044, and 2080 cm^{-1}) of $[Fe_2(bdt)(CO)_6]$, together with the superimposed absorption of the product species that results in peaks at 2035, 1980, and 1890 cm^{-1}. Compared to the IR spectrum of electrochemically generated $[Fe_2(bdt)(CO)_6]^{2-}$ (Figure 1d, blue), the photoinduced product spectrum (Figure 1c, red) is much less red-shifted relative to the parent complex, supporting the assignment of the flash-quench induced absorption changes to the formation of singly reduced $[Fe_2(bdt)(CO)_6]^-$.

The reduction-induced shift of the ν_{C-O} bands by ∼50 cm^{-1} per electron is well in agreement with the IR spectra derived from geometry-optimized DFT calculations (see SI). Earlier studies by Lichtenberger et al.[5a] proposed a bridging coordination of a CO ligand upon 1e$^-$ reduction of $[Fe_2(bdt)(CO)_6]$ on the basis of computational results. However, in our experimental IR spectrum, the lowest frequency band occurs at 1890 cm^{-1}, which would be exceptionally high for a bridging CO ligand in a complex with this ligand set and oxidation state. This expectation is confirmed by our own DFT calculations that predict a ν_{CO} mode at 1791 cm^{-1} for the 1e$^-$ reduced complex with a bridging

dx.doi.org/10.1021/ja5085817 | J. Am. Chem. Soc. 2014, 136, 17366−17369

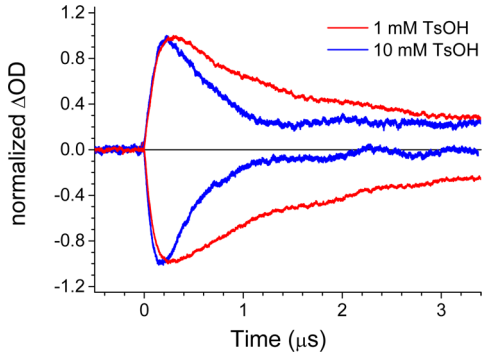

Figure 2. Kinetics of protonation of $[Fe_2(bdt)(CO)_6]^-$ with toluenesulfonic acid. Decay of absorption at 1980 cm^{-1} and recovery of bleaching at 2045 cm^{-1}.

Table 1. Bimolecular Rate Constants for Protonation of $[Fe_2(bdt)(CO)_6]^-$

acid	pK_a[a]	$k_{pt}/M^{-1}\ s^{-1}$
chloroacetic acid	15.3	$<10^6$
trifluoroacetic acid	12.7	7×10^6
trichloroacetic acid	10.6	4×10^6
toluenesulfonic acid	8.7	2×10^8

[a]In acetonitrile solution.[11]

CO ligand. Our DFT results further revealed an alternative geometry of the $1e^-$ reduced complex that features a largely elongated Fe−S bond (by 1.25 Å) but all-terminal coordination of the CO ligands (SI). The computed energy for the latter structure is only slightly lower (~3 kJ/mol) than for the CO-bridged isomer. Comparing computed vibrational stretching frequencies for both structures (SI, Table S-2, Figure S-29) with the experimental IR spectrum, we can safely conclude that the singly reduced state $[Fe_2(bdt)(CO)_6]^-$ is characterized by a rather asymmetric structure with one Fe−S bond broken, but all CO ligands remaining in the terminal position. Only for the second reduction does the experimental IR spectrum of $[Fe_2(bdt)(CO)_6]^{2-}$ clearly indicate a bridging CO at 1682 cm^{-1} (Figure 1d). This assignment is in agreement with DFT calculations (SI) that predict the shift of one CO ligand to a bridging position, while the elongated Fe−Fe distance further increases by 0.35 Å compared to the singly reduced state.

The straightforward generation of $[Fe_2(bdt)(CO)_6]^-$ by the flash-quench method also enabled investigation of its reactivity toward protonation. When $[Fe_2(bdt)(CO)_6]^-$ was generated in the presence of acids, the decay of absorption by $[Fe_2(bdt)(CO)_6]^-$ was increasingly accelerated with increasing acid concentration, as shown in Figure 2. The observed pseudo-first-order rate constants are proportional to acid concentration (SI), and the resulting second-order rate constants k_{pt} for the reaction of $[Fe_2(bdt)(CO)_6]^-$ with several acids are compiled in Table 1.

Protonation could be observed with acids with $pK_a \leq 12.7$, but the rate constant remained well below diffusion-controlled, even for toluenesulfonic acid ($pK_a = 8.7$), which is in line with the nature of this reaction, i.e., oxidative addition to the metal centers. Chloroacetic acid (0.3 M, $pK_a = 15.3$) did not react with $[Fe_2(bdt)(CO)_6]^-$ on the time scale of recombination, putting an upper limit on the order of $10^6\ M^{-1}\ s^{-1}$ on the protonation rate constant. If it is alternatively assumed that protonation fails for thermodynamic reasons, approximate limits for the acidity of

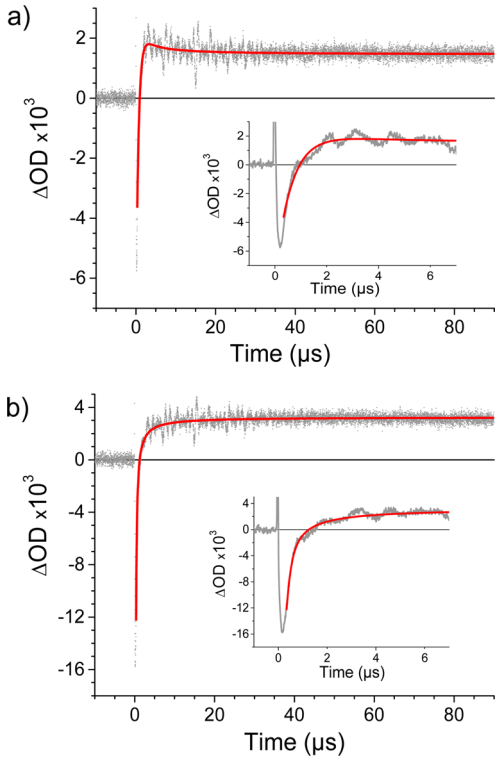

Figure 3. Kinetics of protonation of $[Fe_2(bdt)(CO)_6]^-$ with toluenesulfonic acid (7.4 mM) and subsequent recombination of $[Fe_2(bdt)(CO)_6H]$ with TTF^+ monitored at (a) 2041 and (b) 2047 cm^{-1}. The oscillations clearly visible on the time scale of the insets are due to acoustic waves generated by the actinic laser flash.

$[Fe_2(bdt)(CO)_6H]$ ($9 \leq pK_a \leq 11$) could be estimated,[12] in which the lower limit for the pK_a is in agreement with earlier estimates.[5]

The protonation reactions result in all cases in complete recovery of the bleached absorption bands of $[Fe_2(bdt)(CO)_6]$ but do not give rise to obvious additional absorption features. This indicates that the IR absorption spectrum of the protonation product $[Fe_2(bdt)(CO)_6H]$ must be very similar to the spectrum of $[Fe_2(bdt)(CO)_6]$,[13] which is supported by DFT calculations (SI). Evidence for a slight spectral shift could, however, be obtained from close inspection of the transient absorption changes at the edges of the band at 2044 cm^{-1}. The initial bleach due to reduction of $[Fe_2(bdt)(CO)_6]$ to $[Fe_2(bdt)(CO)_6]^-$ is rapidly recovered in ~1 μs, as shown in the insets in Figure 3. This rapid recovery due to protonation of the reduced catalyst is then followed by slow recombination of $[Fe_2(bdt)(CO)_6H]$ with TTF^+, as shown in the full-sized traces in Figure 3. The recombination process is observed over the first 20 μs as a rise at 2041 cm^{-1} and corresponding decay at 2047 cm^{-1}, indicating a slight red-shift of the band in $[Fe_2(bdt)(CO)_6H]$ as compared to $[Fe_2(bdt)(CO)_6]$. The residual offset of the IR absorption traces arises at least partly from a baseline shift triggered by the actinic laser flash that is seen throughout the spectral region examined (SI, Figure S-15), and hence it provides no reliable measure of the extent of recombination. Analogous measurements with UV/vis detection indicate that a minor fraction of the TTF^+ radical escapes recombination, while no reduced catalyst prevails on this time scale (SI, Figure S-21). Regeneration of $[Fe_2(bdt)(CO)_6]$ by reactions other than recombination with TTF^+ could be a sign of catalytic turnover via a bimolecular reaction between two $[Fe_2(bdt)(CO)_6H]$.

dx.doi.org/10.1021/ja5085817 | J. Am. Chem. Soc. 2014, 136, 17366−17369

Regarding the identity and structure of the protonation product, the magnitude of the protonation-induced shift of the CO stretching frequencies provides unambiguous evidence for protonation on the metal centers, as ligand protonations cause significantly smaller spectral shifts. The nearly perfect spectral match between the hydride complex $[Fe_2(bdt)(CO)_6H]$ and $[Fe_2(bdt)(CO)_6]$, including the absence of low-frequency bands from bridging CO ligands, further reveals that the two species feature similarly symmetric ligand sets. The IR data hence indicate that $[Fe_2(bdt)(CO)_6H]$ is characterized by a bridging hydride and two bridging thiolate ligands. The IR data of $[Fe_2(bdt)(CO)_6H]$ as well as the structural features deduced from it are in excellent agreement with results of geometry-optimized DFT calculations (SI).

In summary, our results demonstrate that the combination of laser flash-quench methods with time-resolved infrared spectroscopy facilitates the investigation of intermediates and their transformations in photoinduced catalytic reactions. This applies in particular to routes triggered by one-electron reduction of the catalyst that are essential to the light-driven catalytic mechanism but not always accessible to electrochemical investigations, as in the case of $[Fe_2(bdt)(CO)_6]$. The time-resolved spectroscopic observation of the $1e^-$ reduced catalyst and its protonation product revealed structural characteristics of these key intermediates and yielded kinetic information on discrete steps in the catalytic cycle. The presented method should be directly applicable to the identification of postulated intermediates in the mechanistic characterization of related catalysts. Future work might be able to elucidate, e.g., the role of basic ligand sites in the formation of hydride intermediates as proposed for the biologically relevant azadithiolate (adt = S^--CH_2-NR-CH_2-S^-) analogues, $[Fe_2(adt)(CO)_6]$.[14]

■ ASSOCIATED CONTENT

Supporting Information

Experimental and computational methods, computational results, and complementary time-resolved UV/vis and IR spectroscopic data. This material is available free of charge via the Internet at http://pubs.acs.org.

■ AUTHOR INFORMATION

Corresponding Author

reiner.lomoth@kemi.uu.se

Notes

The authors declare no competing financial interest.

■ ACKNOWLEDGMENTS

This work was supported by the Swedish Research Council, the Swedish Energy Agency, the K&A Wallenberg foundation, the COST Action CM1305 ECOSTBio, and the Max Planck Society for the Advancement of Science. David C. Grills (Brookhaven National Laboratory, Upton, NY) is gratefully acknowledged for valuable technical advice regarding the nanosecond infrared spectroscopy setup.

■ REFERENCES

(1) (a) Cook, T. R.; Dogutan, D. K.; Reece, S. Y.; Surendranath, Y.; Teets, T. S.; Nocera, D. G. *Chem. Rev.* **2010**, *110*, 6474. (b) Eckenhoff, W. T.; Eisenberg, R. *Dalton Trans.* **2012**, *41*, 13004.

(2) (a) Eilers, G.; Schwartz, L.; Stein, M.; Zampella, G.; de Gioia, L.; Ott, S.; Lomoth, R. *Chem.—Eur. J.* **2007**, *13*, 7075. (b) Singh, W. M.; Mirmohades, M.; Jane, R. T.; White, T. A.; Hammarström, L.; Thapper, A.; Lomoth, R.; Ott, S. *Chem. Commun.* **2013**, *49*, 8638. (c) Singh, P. S.; Rudbeck, H. C.; Huang, P.; Ezzaher, S.; Eriksson, L.; Stein, M.; Ott, S.; Lomoth, R. *Inorg. Chem.* **2009**, *48*, 10883. (d) Samuel, A. P. S.; Co, D. T.; Stern, C. L.; Wasielewski, M. R. *J. Am. Chem. Soc.* **2010**, *132*, 8813. (e) Guo, Y.; Wang, H.; Xiao, Y.; Vogt, S.; Thauer, R. K.; Shima, S.; Volkers, P. I.; Rauchfuss, T. B.; Pelmenschikov, V.; Case, D. A.; Alp, E. E.; Sturhahn, W.; Yoda, Y.; Cramer, S. P. *Inorg. Chem.* **2008**, *47*, 3969. (f) Cheah, M. H.; Tard, C.; Borg, S. J.; Liu, X.; Ibrahim, S. K.; Pickett, C. J.; Best, S. P. *J. Am. Chem. Soc.* **2007**, *129*, 11085. (g) Ezzaher, S.; Capon, J.-F.; Gloaguen, F.; Pétillon, F. Y.; Schollhammer, P.; Talarmin, J.; Pichon, R.; Kervarec, N. *Inorg. Chem.* **2007**, *46*, 3426. (h) Mejia-Rodriguez, R.; Chong, D.; Reibenspies, J. H.; Soriaga, M. P.; Darensbourg, M. Y. *J. Am. Chem. Soc.* **2004**, *126*, 12004. (i) O'Hagan, M.; Shaw, W. J.; Raugei, S.; Chen, S.; Yang, J. Y.; Kilgore, U. J.; DuBois, D. L.; Bullock, R. M. *J. Am. Chem. Soc.* **2011**, *133*, 14301.

(3) (a) Jablonskyte, A.; Wright, J. A.; Fairhurst, S. A.; Peck, J. N.; Ibrahim, S. K.; Oganesyan, V. S.; Pickett, C. J. *J. Am. Chem. Soc.* **2011**, *133*, 18606. (b) Dempsey, J. L.; Winkler, J. R.; Gray, H. B. *J. Am. Chem. Soc.* **2010**, *132*, 16774.

(4) Streich, D.; Astuti, Y.; Orlandi, M.; Schwartz, L.; Lomoth, R.; Hammarström, L.; Ott, S. *Chem.—Eur. J.* **2010**, *16*, 60.

(5) (a) Felton, G. A. N.; Vannucci, A. K.; Chen, J.; Lockett, L. T.; Okumura, N.; Petro, B. J.; Zakai, U. I.; Evans, D. H.; Glass, R. S.; Lichtenberger, D. L. *J. Am. Chem. Soc.* **2007**, *129*, 12521. (b) Capon, J.-F.; Gloaguen, F.; Schollhammer, P.; Talarmin, J. *J. Electroanal. Chem.* **2006**, *595*, 47.

(6) Grills, D. C.; Cook, A. R.; Fujita, E.; George, M. W.; Preses, J. M.; Wishart, J. F. *Appl. Spectrosc.* **2010**, *64*, 563.

(7) For the first and second reduction of $[Fe_2(bdt)(CO)_6]$, DFT calculations (SI) yield reduction potentials of $E_1^\circ = -1.42$ V and $E_2^\circ = -1.21$ V, respectively (vs Fc/Fc^+ in acetonitrile). The average potential is well in accordance with the experimentally observed value of −1.32 V (ref 5a) for the $2e^-$ reduction of $[Fe_2(bdt)(CO)_6]$.

(8) Orain, C.; Quentel, F.; Gloaguen, F. *ChemSusChem* **2014**, *7*, 638.

(9) The rate constant (7×10^{10} M^{-1} s^{-1}) obtained from the transient absorption data even somewhat exceeds the theoretical limit for diffusional recombination of the ions in acetonitrile. This dicrepancy can be attributed to the inhomogeneous transient concentrations generated by the laser flash. While irrelevant for first- and pseudo-first-order kinetics, this effect leads to generally less accurate rate constants for second-order processes (recombinations).

(10) Triethanolamine was used as sacrificial electron donor in combination with $[Ir(ppy)_2(bpy)]^{3+}$ (ppy = 2-phenylpyridine; bpy = 2,2′-bipyridine) as photosensitizer.

(11) Izutsu, K. *Acid-Base Dissociation Constants in Dipolar Aprotic Solvents*; Blackwell: Oxford, 1990.

(12) The upper and lower limits were estimated from the pK_a of chloroacetic acid and trifluoroacetic acid, respectively. For both estimates, the highest excess of chloroacetic acid (0.3 M) and the lowest excess of trifluoroacetic acid (30 mM) over reduced catalyst (ca. 2 μM) were taken into account.

(13) Analogous measurements with UV/vis detection (SI) indicate that also the UV/vis spectra of $[Fe_2(bdt)(CO)_6]$ and $[Fe_2(bdt)(CO)_6H]$ are very similar.

(14) (a) Ott, S.; Kritikos, M.; Åkermark, B.; Sun, L.; Lomoth, R. *Angew. Chem., Int. Ed.* **2004**, *43*, 1006. (b) Berggren, G.; Adamska, A.; Lambertz, C.; Simmons, T. R.; Esselborn, J.; Atta, M.; Gambarelli, S.; Mouesca, J. M.; Reijerse, E.; Lubitz, W.; Happe, T.; Artero, V.; Fontecave, M. *Nature* **2013**, *499*, 66. The catalytic mechanism for complexes with the adt-type bridging ligand has been recently revisited, and indications for proton-directing pendant base effects were indirectly obtained from increased electrocatalytic activity: (c) Bourrez, M.; Steinmetz, R.; Gloaguen, F. *Inorg. Chem.* **2014**, *53*, 10667. (d) Crouthers, D. J.; Denny, J. A.; Bethel, R. D.; Munoz, D. G.; Darensbourg, M. Y. *Organometallics* **2014**, *33*, 4747.